Observation of "Mesh" and "Strut" Structures in Block Copolymer/Homopolymer Mixtures

Takeji Hashimoto,* Satoshi Koizumi, and Hirokazu Hasegawa

Department of Polymer Chemistry, Faculty of Engineering, Kyoto University, Kyoto 606, Japan

Tatsuo Izumitani

Research Center, Daicel Chemical Industries, Ltd., 1239, Shinzaike, Aboshi-ku, Himeji, Hyogo 671-12, Japan

Stephen T. Hyde

Department of Applied Mathematics, Research School of Physical Science, Australian National University, Box 4, Canberra, Australia

Received July 31, 1991; Revised Manuscript Received November 5, 1991

ABSTRACT: "Mesh" and "strut" microdomain structures were observed in a copolymer/homopolymer mixture. The mesh structure consists of alternating parallel sheets composed of A and B macromolecules in which one type of sheets (e.g., A) is fused by catenoidal channels of A traversing through the other type of sheets B. The strut structure is a three-dimensional tunnel network characteristic of bicontinuous microdomain structures of A and B. The mesh and strut structures consist mostly of a hyperbolic interface (with negative Gaussian curvature). They were found between the lamellar and spherical phases.

I. Introduction

The study of self-assembly in block copolymer systems has received considerable impetus recently with reports of a bicontinuous phase in pure copolymer systems in both linear and star architecture diblock copolymers.[1,2] This phase lies between the standard lamellar and cylindrical phases and consists of two interpenetrating diamond networks of the minor block chains, separated by a continuous matrix of the major phase, which lines the periodic minimal surface known as the D-surface.[3]

Standard theories of block copolymer self-assembly have failed to predict the presence of this phase, although recent work[4] suggests that the formation of hyperbolic (saddle-shaped) interfaces is possible in copolymer systems. One of us (S.T.H.) has developed a simple theory[5] of self-assembly of pure block copolymer melts in the strong segregation limit which suggests that the formation of a hyperbolic interface is possible between the lamellar and spherical phases.

The formation of bicontinuous structures (more accurately termed multicontinuous) in these systems is analogous to the formation of cubic phases in surfactant/water mixtures, which occurs at intermediate compositions to those required for the formation of lamellar and (hexagonal) cylindrical phases. In surfactant systems, a further hyperbolic interface between polar and hydrophobic regions has been found, namely, what we term a "mesh" structure, which consists of pairs of parallel sheets, fused by catenoids which form a regular two-dimensional square or hexagonal lattice.[6] In this way, planar tunnel networks are created between the pairs of sheets, which are stacked over each other to form three-dimensional tetragonal or rhombohedral structures. In topological terms, these mesh structures are intermediate to stacks of parallel plates and the three-dimensional tunnel networks characteristic of bicontinuous structures (which we call "strut" structures, in contrast to the two-dimensional networks characteristic of mesh structures). Recently a theory for the mesh phases was presented by Fredrickson,[7] again for pure block copolymer melts.

Although the theories described above deal with the hyperbolic interfaces for pure copolymer melts, there are no theories for the hyperbolic interfaces for the blends of block copolymer/homopolymer systems. We extended the studies of the self-assembly of pure copolymer melts to those of blends of a copolymer with a homopolymer. The blends are physically quite different from the pure copolymer melts, and their self-assembled patterns are expected to be even richer than those for pure copolymers, simply because the blended homopolymers may be able to be localized in the regions with a high interfacial curvature. In this paper we report experimental studies of both mesh and strut structures in a copolymer/homopolymer system.

II. Experimental Methods

1. Samples. As a block copolymer K-Resin (KR-03, Phillips Petroleum Co.) was used in this work. This commercially available block copolymer consists of 24 wt % butadiene and 76 wt % styrene segments characterized by IR spectroscopy and has number- and weight-average molecular weights 8.0×10^4 and 1.57×10^5, respectively, evaluated by size-exclusion chromatography. We were informed that this polymer has a star-shaped molecular architecture, with an average of about four arms, with each arm consisting of a diblock copolymer of polybutadiene and polystyrene. The polystyrene homopolymer to be added to this block copolymer was TS23 (number-average molecuar weight and polydispersity index being 2.8×10^3 and 1.05, respectively) which was also commercially available and supplied by TOSOH Co., Ltd.

2. Film Preparations. KR-03 and TS23 were mixed in nine different ratios (KR-03/TS23 = 100/0, 90/10, 80/20, 70/30, 60/40, 50/50, 40/60, 30/70, and 20/80 by weight) and dissolved in toluene, which is a neutral solvent. Film specimens ca. 0.3 mm thick were prepared by casting 5.0 wt % toluene solution in Petri dishes. The solvent was slowly evaporated over 10 days at 30 °C. The film specimens thus prepared were further dried in a vacuum oven at room temperature until a constant weight was attained.

3. Transmission Electron Microscopy. The as-cast film specimens were stained with osmium tetroxide vapor and embedded in epoxy resin. The samples were then subjected to ultramicrotoming into ultrathin sections ca. 50 nm thick. Ul-

0024-9297/92/2225-1433$03.00/0

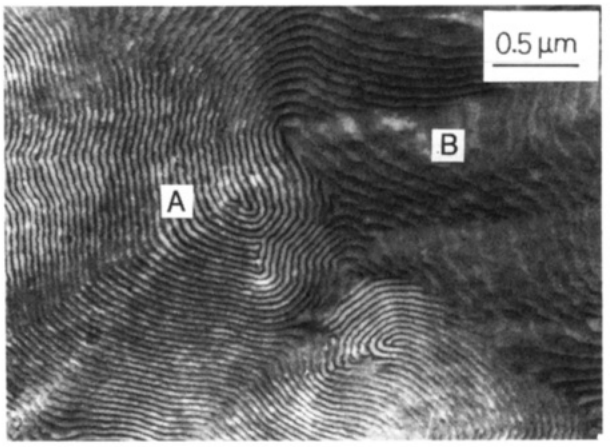

Figure 1. Electron micrograph of an ultrathin section of neat KR-03 film cast from toluene solution. The section was stained with osmium tetroxide. The regions marked A and B correspond to those of lamellae with a different orientation with respect to the thin section, as shown in Figure 2.

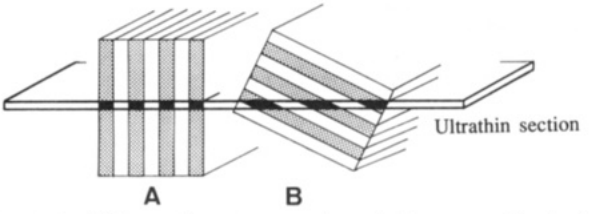

Figure 2. Schematic representation of the geometrical relationship between lamellar microdomains in the cast film of neat KR-03 and an ultrathin section. Portion A contains a normal section of the lamellae, but portion B contains an oblique section.

trathin sections parallel and perpendicular to the film surfaces were investigated to obtain the information on the three-dimensional structures. The ultrathin sections were further subjected to the staining by osmium tetroxide vapor on a microscope grid before the transmission electron microscopic (TEM) investigation with a Hitachi H-600S transmission electron microscope operated at 100 kV.

III. Experimental Results

Figure 1 shows an electron micrograph of an ultrathin section of neat KR-03 film cast from toluene solution. The dark regions correspond to polybutadiene (PB) microdomains selectively stained with osmium tetroxide, and the bright region corresponds to the unstained polystyrene (PS) microdomains. The pattern resembles "wood grain". The striations with a regular spacing of ca. 35 nm are observed in region A in the left half of the micrograph. The micrograph suggests a microdomain structure of lamellar morphology composed of PS and PB lamellar microdomains. Such a TEM image is expected for the portion of the ultrathin section cut normal to the lamellar interfaces as schematically shown in portion A in Figure 2. The widths of the striations and their spacings in region B in the right half of the micrograph are much larger and more irregular than those in region A. This pattern corresponds to the portion of the ultrathin section cut at an oblique angle to the lamellar interface whose orientation locally varies, as schematically shown in portion B in Figure 2. Although not shown here similar lamellar microdomain structures were observed for KR-03/TS23 90/10 and 80/20 mixtures. Small-angle X-ray scattering further supported the existence of the lamellar microdomains with a long-range spatial order,[8,9] although the prolfiles are not shown here.

Figure 3 shows an electron micrograph of an ultrathin section cut normal to the surface of the thin film cast from a toluene solution of a KR-03/TS23 70/30 mixture. At a glance it resembles the micrograph of the neat KR-03 film with the lamellar microdomain morphology (see Figure 1, region A). However, a high magnification (part b) reveals that the dark striations with a regular spacing of ca. 32 nm are not always solid but rather consist of an array of dark spots. It suggests that the morphology is different from lamellae and that the dark polybutadiene microphase does not form a solid piece of sheet. The micrograph containing a part of the free surface of the cast film,[10] though not shown here, implied that the microdomains in the as-cast films tend to align highly oriented parallel to the film surfaces as found for the lamellar microdomains in the solvent-cast films.[8]

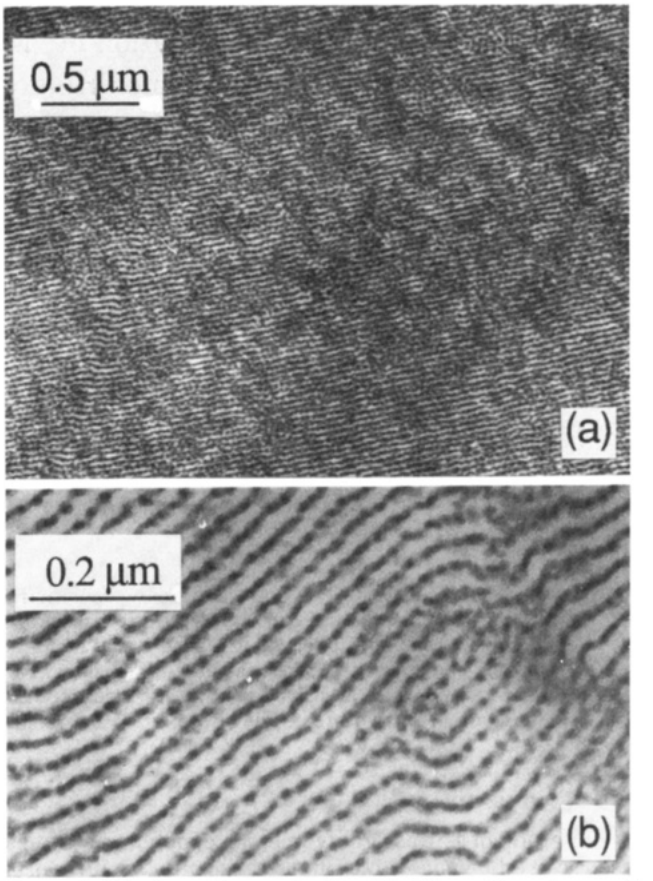

Figure 3. Electron micrograph of an ultrathin section cut normal to the surface of the thin film cast from a toluene solution of a KR-03/TS23 70/30 mixture. (a) Low magnification. (b) High magnification.

Figure 4 shows the TEM micrograph obtained on the ultrathin section cut parallel to the surface of the same film specimen. The TEM image in Figure 4 is significantly different from that in Figure 3. The image comprises a series of dark and bright onion-ring-type patterns schematically shown in Figure 5a on which a fine mesh-type pattern as sketched in Figure 5b is superimposed. The onion-ring-type pattern is interpreted as that expected for the ultrathin section cut through the bent layers of PS and PB, shown schematically in Figure 5c. Note that thickness t of the thin section relative to that of the spacing D is not necessarily correctly sketched in part c, but t/D in the sketch was chosen in order to help in highlighting the onion-ring-type image. The mesh-type pattern may then reflect a fine structure existing in the PB layers. Since the interfaces of the layers are preferentially oriented parallel to the film surfaces, the TEM image as shown in Figure 4 is more often observed in the section cut parallel to the film surfaces than in that cut normal to them.

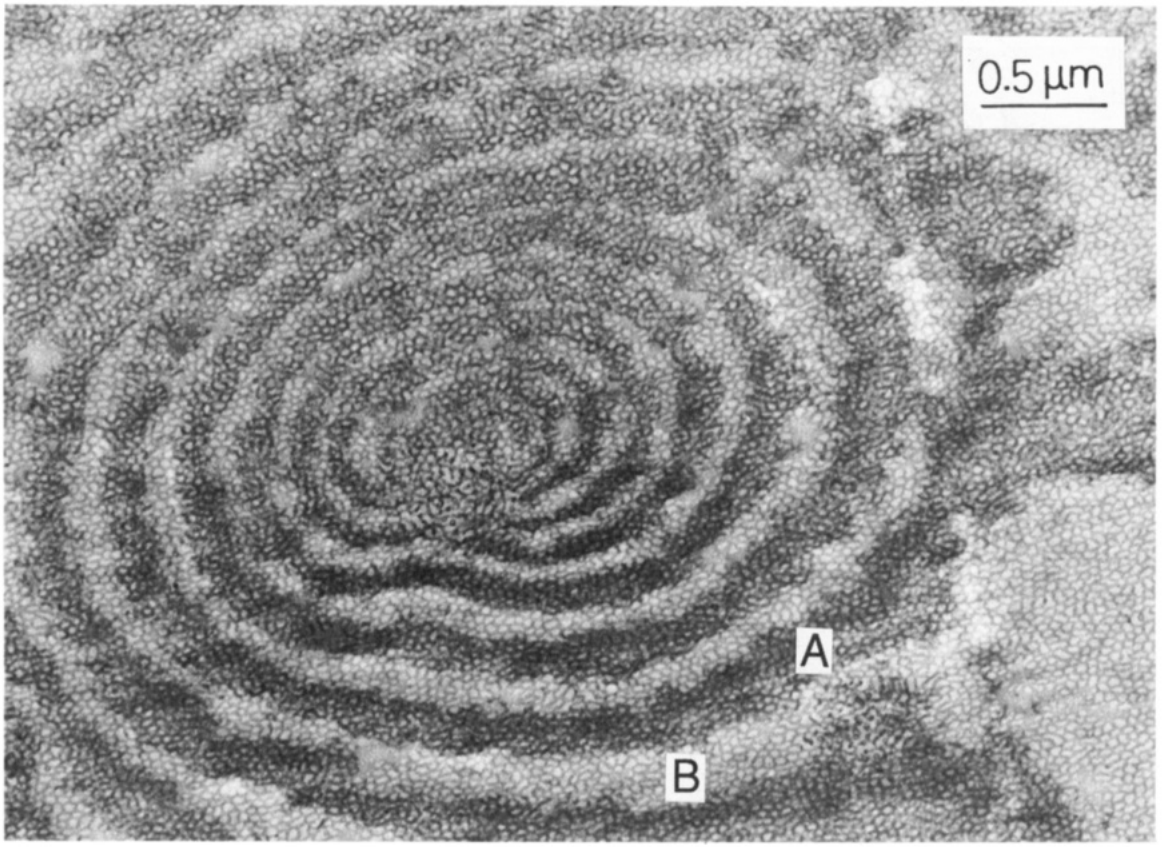

Figure 4. Electron micrograph of an ultrathin section cut parallel to the surfaces of the same film specimen as Figure 3.

In order to interpret properly the meshlike image in Figure 4, it is extremely important to consider overlap of the images originating from the PB mesh layers and featureless PS layers along the thickness direction of the ultrathin section. This is because the periodicity in the direction normal to the mesh layer is 30 nm, the thickness of the featureless PS layer is about 20 nm according to SAXS results,[9] and that of the ultrathin section is about 50 nm or more. Thus the thin section contains at least one mesh layer of PB, two mesh layers or more in some portions, when it is cut more or less parallel to the interface between the PB and PS layers. In order to have only PS domains in an ultrathin section cut parallel to the interface, its thickness must be controlled less than 20 nm, which is almost impossible by using current techniques. On the othe rhand, featureless PS domains can be easily observed in the ultrathin sections cut normal to the plane of the interfaces between the two layers as shown in Figure 3. In this case an increase of the thickness t allows us to detect the featureless PS layer (i.e., pure PS domains uncontaminated by PB segregations) over a wide region along the thickness direction or parallel to the interface. This result increased our confidence in the morphology composed of the featureless PS layer and PB mesh layer as a repeating unit.

The mesh-type pattern is seen to be the spotlike bright PS microdomains dispersed in the dark PB matrix, as shown in region A in the micrograph in Figure 4 and in the sketch in Figure 5a, or the dark meshlike domains of PB in the bright matrix of PS, as shown in region B in the micrograph and in the sketch in Figure 5b. The latter image may reflect the image for the portion of the thin section containing only one PB mesh layer along the thickness direction and result from a superposition of the pattern in the dark PB mesh phase and the featureless bright PS phase. On the other hand, the former image may reflect the one for the portion of the thin sections containing two or more PB meshes along the thickness direction and result from a superposition of the two mesh images or more. From these observations, we propose, as a possible morphology, a microdomain structure composed of alternating layers of solid PS microdomains and PB microdomains as sketched in Figure 6a, but the PB layers have the meshlike structure with their holes filled with PS block polymers and homopolymers, as sketched in parts b and c of Figure 6, as possible models. Thus the mesh structure is considered to be a one-dimensional periodic stack of the PB mesh, stacked parallel to the z-axis in Figure 6a, in the matrix of the PS domain. The PS domain is three-dimensionally continuous through the PS holes or channels in the PB mesh-type domains, but the PB domains are continuous only in two dimensions.

The PB mesh in the sample shown in Figure 4 (especially in region B of the micrograph) consists almost exclusively of six-membered rings with nodes connecting three PB tunnels at each ring vertex. A part of the nodes are marked by the symbol × in part b of Figure 6. Distortions of the ring geometries result in a disordered array of PS channels, although the mesh architecture is topologically identical to a regular hexagonal tiling of the plane. It is not known whether these distortions occur during the ultrathin sectioning or whether they are inherent in the bulk sample. We tend to believe the latter interpretation is more likely than the former. The distortions in this case may be attributed to polydispersities of the block copolymer used in this study in terms of molecular weight, composition, and arm numbers. The intrinsic characteristics of the block copolymer may, in turn, cause local concentration fluctuations of the homopolystyrene and hence the fluctuation in the PS channel size.

The sample may consist of disordered mesh layers, or the PS channels in the PB mesh may have a local order of two-dimensional rhombohedral symmetry as sketched in Figure 6b or tetragonal symmetry as sketched in Figure

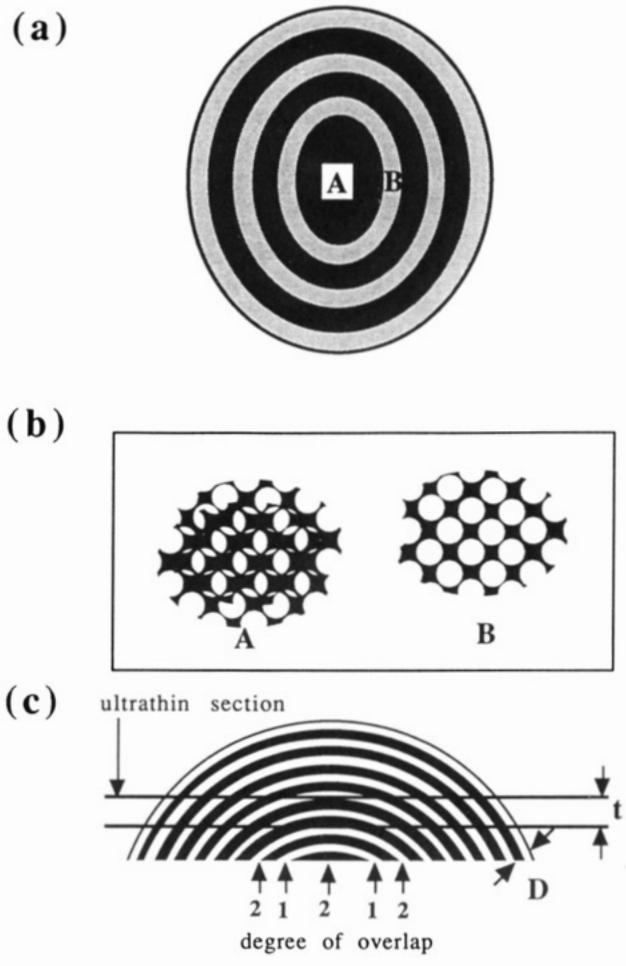

Figure 5. Schematic representation of (a) an onion-ring-type pattern comprising a series of the dark (A) and bright striations (B), (b) a fine mesh-type pattern in the dark (A) and bright striations (B), and (c) a geometrical relationship between onion-ring-type layered microdomain structure of the cast film of a KR-03/TS23 70/30 mixture and the ultrathin section.

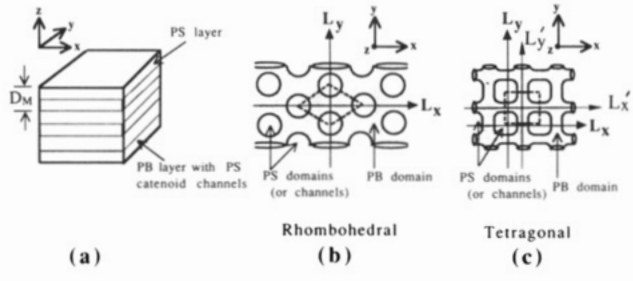

Figure 6. Schematic representation of (a) a lamellalike stack of solid PS layers and PB layers with PS catenoid channels, (b) a PB mesh with two-dimensional rhombohedral symmetry, and (c) a PB mesh with two-dimensional tetragonal symmetry.

6c. The rhombohedral and tetragonal symmetries are obtained by deformation of different minimal surfaces, the D-surface and P-surface, respectively. The simplest models of the mesh morphology are sketched in Figure 6. (Of course, more complex two-dimensional nets are also possible, so that a range of three-dimensional symmetries can occur.) The TEM image shown in Figure 3 may be the one observed for the ultrathin section cut through the planes parallel to the z-axis in Figure 6. The fine structure in the dark PB layers which appear as arrays of dark circles may be observed for the ultrathin section cut through the planes parallel to the z-axis and containing the lines L_x or L_y in parts b and c of Figure 6. When the ultrathin sections are cut through the plane containing the z-axis and L'_x (or L'_y), the dark layers will become continuous but their thicknesses, and hence contrast, will vary, as seen in some part of the micrograph shown in the Figure 3 and as will be discussed in Figure 9 (the layer C_1). The fine structure may suggest that the PS channels have a catenoidal shape. The mesh-type morphology as observed in Figure 4 may be obtained for the TEM observation with the ultrathin section cut more or less normal to the z-axis. The different appearance in the mesh-type morphology between regions A and B in Figures 4 and 5b may be related to the orientation of the mesh with respect to the ultrathin section and overlap of the mesh layers along its thickness direction as sketched in Figure 5c: regions A may correspond to those where two PB meshes overlap along the thickness direction of the thin section and regions B to those where only a single PB mesh exists.

A similar microdomain structure to this mesh morphology has been inferred by Matsuo and Sagaye.[11] They observed the ultrathin sections normal and parallel to the film surfaces by TEM for a poly(styrene-*block*-butadiene-*block*-styrene) triblock copolymer with a styrene/butadiene molar ratio of 80/20 cast from cyclohexane solution and found the PB component forming a rough network which piled up one after another in the matrix of the PS component. However, from their reported micrographs alone, it seems difficult to identify unequivocally the structure reported by them as the mesh structure. The lamellar catenoid reported by Thomas et al.[4] is at first sight similar to this mesh morphology. However, in the former the catenoid channels traverse both layers, so that both domains are three-dimensionally continuous, resulting in a strut morphology.

Figure 7a is an electron micrograph of an ultrathin section of a KR-03/TS23 60/40 mixture film cast from a toluene solution. In this micrograph, the dark polybutadiene microphase seems to form, more or less, flexible cylindrical structures which are linked to each other to form a three-dimensional percolation network in a polystyrne matrix, therefore, a bicontinuous three-dimensional network structure or a strut structure. The interfaces between the links may be hyperbolic in nature. Three-dimensional continuity of the polybutadiene phase with hyperbolic interfaces can be easily deduced from contrast variation of the dark PB microdomains. For example, the darker spots marked by white arrows in the micrograph which correspond to the cross sections of the cylindrical units oriented normal to the ultrathin section (see PB microdomain A in Figure 7b). Such cylindrical units with the normal orientation (the domain A) should have a larger dimension in the thickness direction of the ultrathin section than those orienting parallel to the surface of the ultrathin section (the domain B in Figure 7b) and hence appear darker in the micrograph (as sketched in Figure 7c). The hyperbolic interfaces are clearly seen in the portions where the networks are linked. The diameters of the cylindrical units of polybutadiene microdomains and the characteristic size of the cylindrical network seem to be quite uniform. However, a crystallographic order as in the case of OBDD[1,2] was not observed here. A similar struct structure was also reported by Schwier et al. for a mixture of three kinds of poly(styrene-*block*-butadiene) diblock copolymers, and they showed an excellent mechanical property.[12]

Upon further addition of polystyrene homopolymer to the mixture KR-03/TS23, the microdomain morphology of the films cast from a toluene solution changed from a 3D network of PB to spherical microdomains of PB dispersed in a PS matrix,[9] in accord with Molau's rule.[13]

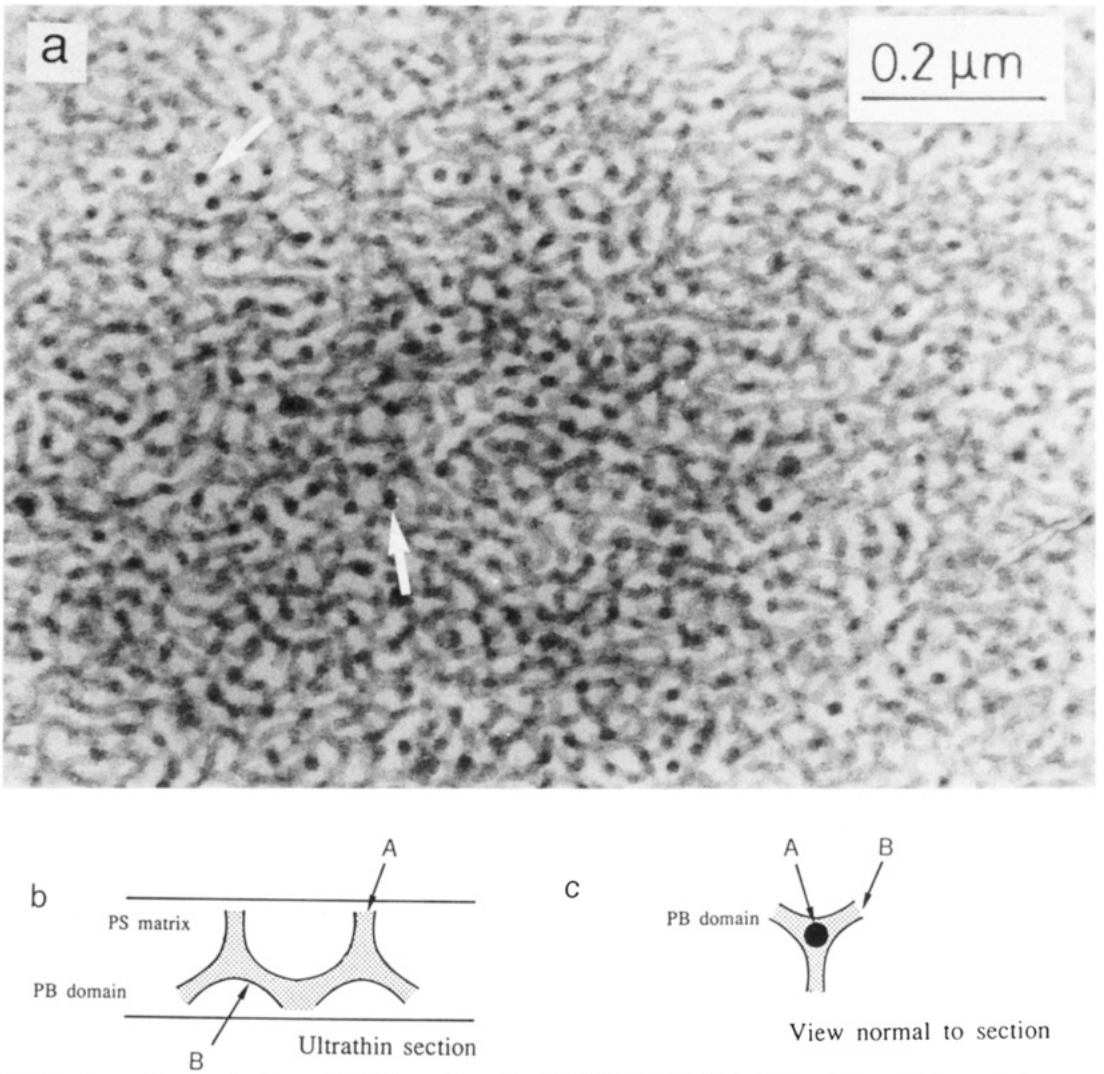

Figure 7. (a) Electron micrograph of an ultrathin section of a KR-03/TS23 60/40 mixture film cast from a toluene solution. (b) Schematic diagram showing a part of the PB network oriented normal (A) and nearly parallel (B) to the ultrathin section. (c) Schematic diagrams showing the contrast distribution of the structure b under TEM observations.

Therefore, the mesh and strut structures were observed in the composition range of the mixture between lamellar and spherical morphologies. The distortion of the mesh and strut structures may have the same origin and may be due to intrinsic characteristics of bulk structure, which in turn originates from intrinsic characteristics of the copolymer and the resulting local concentration fluctuations of the homopolymer as discussed earlier in this section.

IV. Discussion

The details of the model used to understand copolymer self-assembly will be presented elsewhere.[5] An intuitive picture of the physics underlying copolymer self-assembly runs as follows. If the radii of gyration of the two moieties differ, some stretching of (at least) one of the blocks must occur in order to pack the microphases at uniform density. Since the stretching deformation has induced substantial anisotropy into the polymer chains, the conformational entropy of the chains is reduced. Some of this entropy loss can be restored by curving the interface, thereby reducing the anisotropy. Explicit expressions for the free energy of the system as a function of the interfacial curvatures have been obtained by generalizing the analysis of Jackson, Shen, and MacQuarrie[14] to deformations which alter the curvatures of the material. The theory predicts that hyperbolic interfaces (with principal curvatures of opposite sign) are of identical free energy (within 1%) to cylindrical interfaces in diblock assemblies at about 45% by volume of minor component (assuming an equal segment length for both blocks). The situation with added homopolymer is similar, although results are preliminary.

The origin of this mesh phase is, however, unable to be conclusively modeled at this stage, since both mesh and strut morphologies are of hyperbolic geometry. Nevertheless, some remarks regarding its geometry and relative stability are pertinent. To date, little is known of mesh surfaces. Lawson[15] established that crystalline versions of these surfaces can be realized as constant mean curvature (cmc) surfaces, although explicit parametrization of cmc mesh surfaces is impossible at present. Note, however, that these surfaces cannot be minimal surfaces (i.e., zero mean curvature), since minimal surfaces cannot be confined between two planes.[16]

Mesh surfaces are simpler than strut surfaces (which include triply-periodic minimal surfaces), since their genus per unit cell can be as low as two, while strut surfaces must have a genus per unit cell of at least three. (The genus of a surface is related to the number of handles or tunnels in the surface.) In topological terms then, the occurrence of a mesh morphology between lamellar and strut morphologies is not surprising.

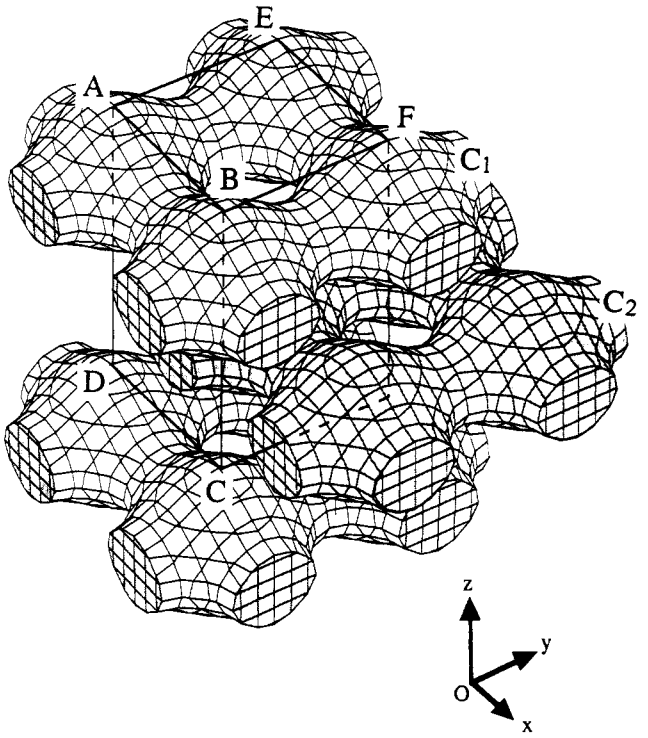

Figure 8. Computer graphics of a homogeneous global embedding of mesh surfaces with a constant mean curvature forming a three-dimensional lattice of body-centered tetragonal symmetry. The graphics was generated by using eq 1 with $a = 0.7$ and $b = 1.2$.

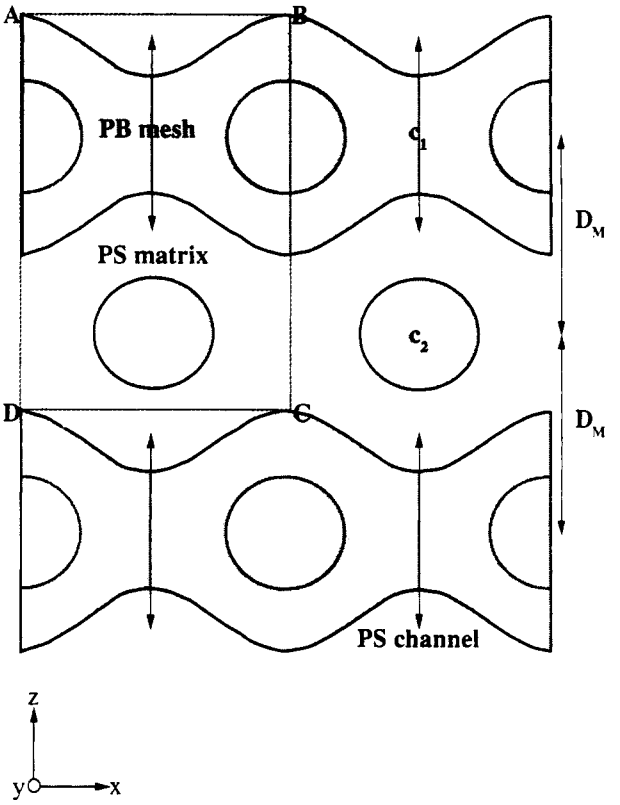

Figure 9. Cross section of Figure 8 cut through the plane ABCD, viewed along the y-axis. The meshes with two-dimensional tetragonal symmetry are stacked in parallel along the Z-direction with a distance D_M.

Theoretical understanding of the stability of this mesh phase is less straightforward. Recent calculations by Fredrickson[7] fail to explain the presence of such a phase in the strong segregation limit of pure diblock copolymers. Our calculations suggest that hyperbolic interfaces are possible in pure copolymer melts, although the global morphology of that interface cannot be predicted. In our view, the occurrence of a particular domain geometry and topology is linked to the variations of curvature and domain thickness required to fill the domains at uniform density, since these variations affect the free energy of copolymer aggregation. The computation of these variations requires explicit Cartesian parametrization of the surface coordinates.[18] Besides the factors mentioned above that contribute to the selection of a particular domain geometry, the architecture of the copolymers, e.g., linear, branched, star, etc., is crucial, as it may modify the configurational entropy of a given structure.

In the case of strut geometries, such calculations can be done assuming the interfaces are parallel surfaces to triply-periodic minimal surfaces. (In the case of the OBDD structure, the relevant minimal surface is the D-surface.) For the mesh morphology, we have the following equation for the square mesh

$$\cos(x) + \cos(y) + \frac{1}{a^2}\cos\left(\frac{z}{a}\right) = \pm b \qquad (1)$$

where $0 < a < 1$ and b is constrained by $\max[-2 + a^{-2}, 2 - a^{-2}] < |b| < a^{-2}$. As the values of the constants a and b are changed, the variations of tunnel radii along the length of the tunnels change.[17] The choice of optimal a and b values for a given composition requires detailed numerical calculations, which are in progress. Note that this equation describes a surface whose mean curvature varies.

In terms of curvature variations, the most homogeneous mesh surfaces are expected to be those whose 2D internal tunnel networks trace out hexagonal and square lattices (parts b and c of Figure 6, respectively), since these have the simplest topology of all two-dimensional networks. In order to form as nearly a uniform distribution of domain identity periods as possible, these mesh sheets are expected to stack into parallel layers, with the tunnel nodes of each layer (e.g., points A, B, E, and F) centered over the pores of neighboring layers as shown in Figure 8. This results in mesh morphologies of body-centered tetragonal (see the unit cell drawn with lines ABFE and ABCD in Figure 8) or rhombohedral symmetry. As yet, we cannot parametrize other mesh surfaces which may be favored for copolymer aggregation. Until the geometry of these surfaces can be better characterized, the origin of the mesh morphology will remain uncertain.

The relative stability of disordered mesh and strut structures compared with crystalline versions, such as the rhombohedral or tetragonal mesh and the OBDD morphology, is impossible to gauge. Unfortunately, no geometric prescription exists for these disordered surfaces. Indeed, the existence of a disordered minimal surface of unbounded topology (which would be an appropriate model for the morphology apparent in Figure 7) is still uncertain, as is the possibility of a disordered cmc mesh surface.

Figure 8 shows computer-generated parallel stacks of the square mesh surfaces plotted from eq 1, with nodes of one layer (e.g., C_1) lying over holes of its neighboring layer (e.g., C_2). The stacks generate a global morphology similar to the classical lamellar phase and hence to the TEM micrographs shown in Figure 3. The meshes can be uniformly stacked to give a global structure with a three-dimensional lattice of body-centered tetragonal symmetry. The cross section of Figure 8 cut through the plane ABCD will have an image as sketched in Figure 9 when viewed

along the y-axis. The shaded regions correspond to the PB meshes C_1 and C_2 in Figure 8 stacked with a distance D_M along the z-axis (a true structural periodicity along the z-axis is $2D_M$). This cross section which comprises the dark layer C_1 with continuous thickness or contrast variations and C_2 with a series of dark domains separated by bright PS domains yields an image similar to that shown in Figure 3.

V. Conclusion

New microdomain morphologies were found between lamellar and spherical microdomains for the mixtures of block copolymer and homopolymer. They are of mesh and strut topologies; the latter has a new bicontinuous microdomain structure other than the OBDD.[1,2] With an increasing amount of homopolymer, morphological transitions from lamellae, mesh, strut to sphere were observed. The presence of both mesh and strut morphologies is, at least, consistent with the theoretically predicted preferred hyperbolic interfacial geometry between lamellar and spherical morphologies for pure copolymer melts but should be further confirmed in the future for the copolymer/homopolymer blends.

Acknowledgment. This work was supported in part by a Grant-in-Aid for Scientific Research in Priority Area "New Functionality Materials, Design, Preparation and Control" (02205066), Ministry of Education, Science and Culture, Japan. S.T.H. thanks the Department of Industry, Technology and Commerce (Australia) for support via a Japan–Australia Cooperative Research Grant. We are grateful to TOSOH Co., Ltd., for providing the TS23 specimen.

References and Notes

(1) Thomas, E. L.; Alward, D. B.; Kinning, D. J.; Martin, D. C.; Handlin, D. L., Jr.; Fetters, L. J. *Macromolecules* **1986**, *19*, 2197.
(2) Hasegawa, H.; Tanaka, H.; Yamasaki, K.; Hashimoto, T. *Macromolecules* **1987**, *20*, 1651.
(3) Anderson, S.; Hyde, S. T.; Larsson, K.; Lidin, S. *Chem. Rev.* **1988**, *88*, 221.
(4) Thomas, E. L.; Anderson, D. M.; Henkee, C. S.; Hoffman, D. *Nature* **1988**, *334*, 598.
(5) Hyde, S. T.; Fogden, A.; Ninhham, B. W., to be published.
(6) Hyde, S. T. *J. Phys. Colloq.* **1990**, *C7*, 209.
(7) Fredrickson, G. H. *Macromolecules* **1991**, *24*, 3456.
(8) Hashimoto, T.; Nagatoshi, K.; Todo, A.; Hasegawa, H.; Kawai, H. *Macromolecules* **1974**, *7*, 364. Hashimoto, T.; Todo, A.; Itoi, H.; Kawai, H. *Macromolecules* **1977**, *10*, 377. Hashimoto, T.; Shibayama, M.; Kawai, H. *Macromolecules* **1980**, *13*, 1237.
(9) Koizumi, S.; Hasegawa, H.; Hashimoto, T., in preparation.
(10) Hasegawa, H.; Hashimoto, T. *Macromolecules* **1985**, *18*, 589; *Polymer*, in press.
(11) Matsuo, M.; Sagaye, S. *Polym. Prepr. (Am. Chem. Soc. Div. Polym. Chem.)* **1970**, *11*, 384.
(12) Schwier, C. E.; Argon, A. S.; Cohen, R. E. *Polymer* **1986**, *26*, 1985.
(13) Molau, G. E. *Block Copolymers*; Aggarwal, S. L., Ed.; Plenum: New York, 1970.
(14) Jackson, J. L.; Shen, M. C.; MacQuarrie, D. A. *J. Chem. Phys.* **1966**, *44*, 2388.
(15) Lawson, H. B. *Ann. Math.* **1990**, *92*, 335.
(16) Hoffman, D. A. *J. Phys. Colloq.* **1990**, *C7*, 197.
(17) Hyde, S. T., unpublished result.
(18) Anderson, D. M.; Thomas, E. L. *Macromolecules* **1988**, *21*, 3221.

Registry No. PS (homopolymer), 9003-53-6.